Supporting Information

Interfacial Energetic Disorder induced by the Molecular Packing Structure at the Conjugated Polymer-based Donor/Acceptor Heterojunction

Ke Zhou,*[,1] *Yuxuan Liu*,[1] *Yunxiang Xu*,[2] *Hongbo Wu*,[3] *Xiaobo Zhou*,[1] *Kai Chen*,[1] *Xiaofeng Xu*,[2] *Zaifei Ma*,[3] *Zheng Tang*,[3] and *Wei Ma* *[,1]

[1]State Key Laboratory for Mechanical Behavior of Materials, Xi'an Jiaotong University, Xi'an 710049, P. R. China

Corresponding author: msekzhou@xjtu.edu.cn, msewma@xjtu.edu.cn

[2]College of Materials Science and Engineering, Ocean University of China, Qingdao 266100, P. R. China

[3]Center for Advanced Low-dimension Materials, State Key Laboratory for Modification of Chemical Fibers and Polymer Materials, College of Materials Science and Engineering, Donghua University, Shanghai 201620, P. R. China

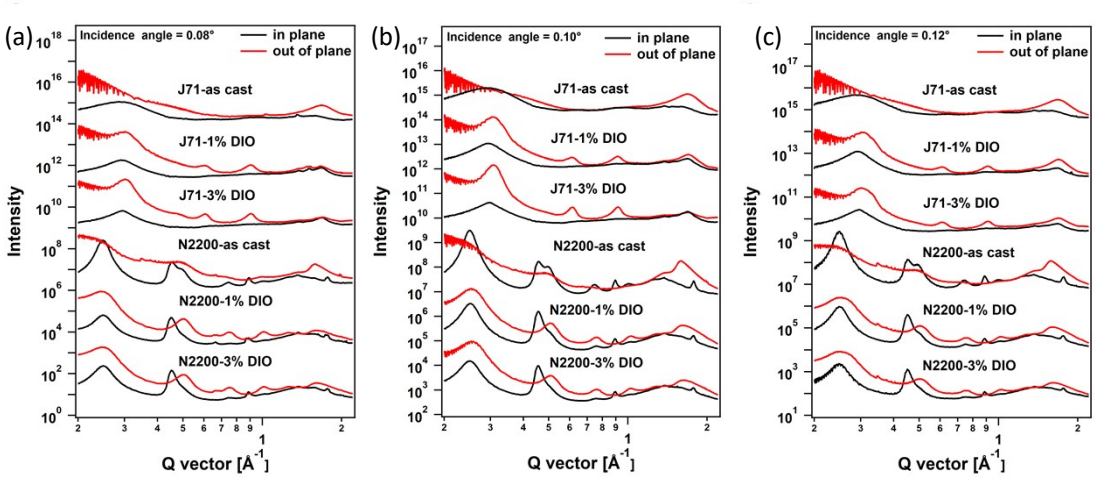

Figure S1 Line cuts of GIWAXS profiles with different grazing incidence angles (a) 0.08°, (b) 0.10°, and (c) 0.12° for J71 and N2200 films.

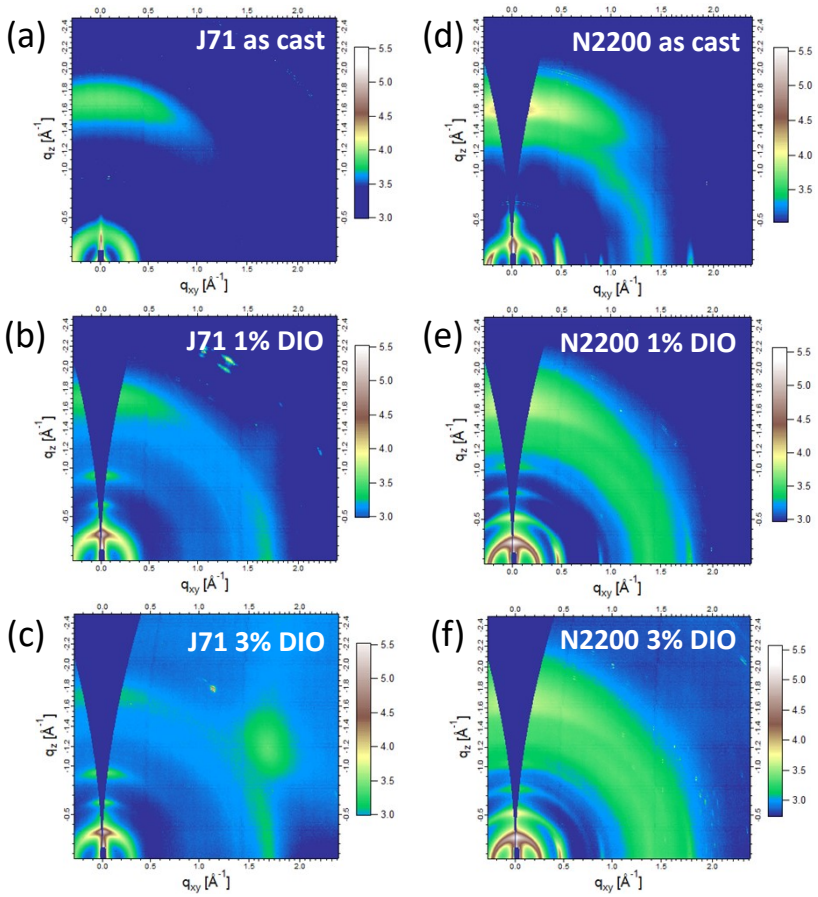

Figure S2. The 2D GIWAXS scattering patterns of pure J71 and N2200 films with different content of DIO.

Table S1. The fitted results based on the GIWAXS for different J71 and N2200 films.

		Location ($Å^{-1}$)	D-spacing (Å)	FWHM	Coherence length(Å)
OOP (010)	J71-as cast	1.68	3.73	0.22	25.34
	J71-1% DIO	1.69	3.72	0.17	33.33
	J71-3% DIO	1.68	3.74	0.17	32.63
	N2200-as cast	1.61	3.91	0.15	37.03
	N2200-1% DIO	1.64	3.82	0.26	21.74
	N2200-3% DIO	1.65	3.81	0.27	21.00
IP(100)	J71-as cast	0.29	21.55	0.11	50.75
	J71-1% DIO	0.29	21.38	0.07	77.86
	J71-3% DIO	0.30	21.22	0.07	80.47
	N2200-as cast	0.25	25.10	0.02	299.15
	N2200-1% DIO	0.25	24.99	0.03	223.81
	N2200-3% DIO	0.25	25.12	0.03	196.35
IP(010)	J71-1% DIO	1.67	3.76	0.17	34.21
	J71-3% DIO	1.68	3.73	0.12	46.64

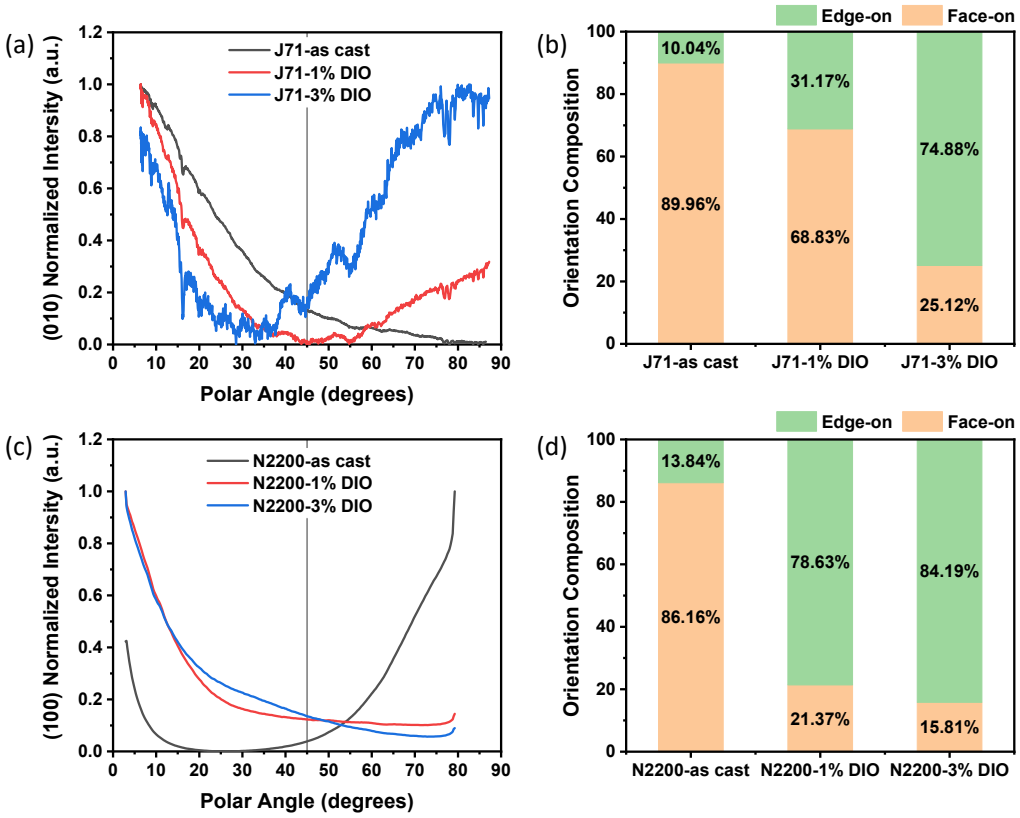

Figure S3. The pole figures of (a) (010) diffraction peak in J71 films and (c) (100) diffraction peak in N2200 films. The amount of face-on and edge-on orientation is also calculated for (c) J71 and (d) N2200 films.

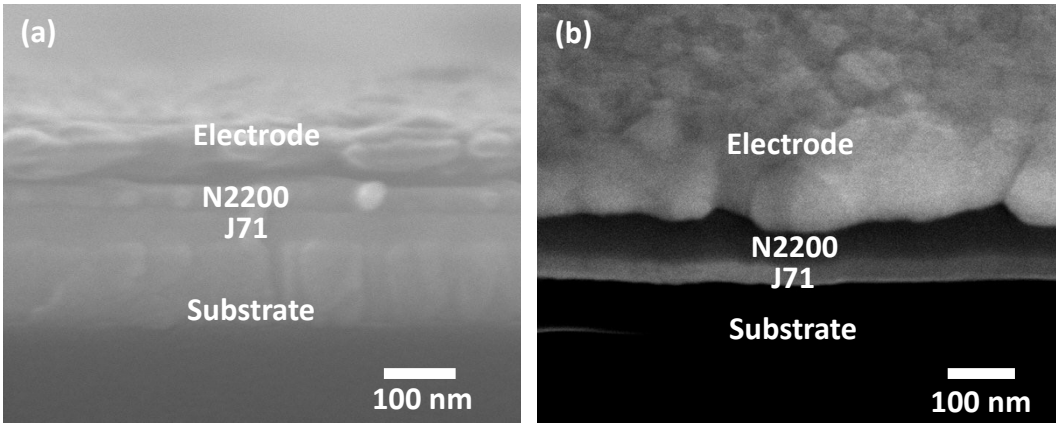

Figure S4. The cross-section morphology of J71/N2200 bilayer recorded using (a) scanning electron microscopic (SEM) and (b) focused ion-beam (FIB) microscopic.

The cross-section image (a) is recorded with the SEM (SU6600, HITACHI) and the bilayer sample is prepared by breaking it in the liquid nitrogen. The cross-section is subjected to gold spray so as to improve its electronic conductivity before characterization. The cross-section image (b) is recorded by a FIB microscopic (09CERNET MM3A-EM) with a tilt angle of 52^{o}. Both of the images exhibit the sharp interface between J71 and N2200 layers, suggesting that the bilayer structure is well retained using the PDMS-transfer method.

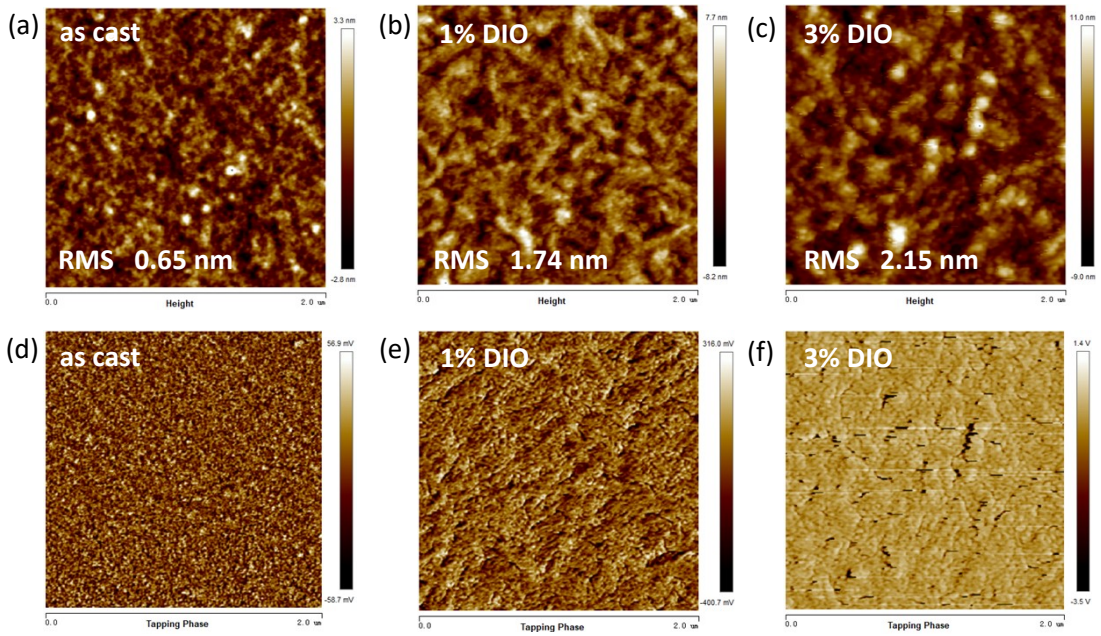

Figure S5. The surface height (a-c) and phase images (d-f) for pure J71 films with different content of DIO.

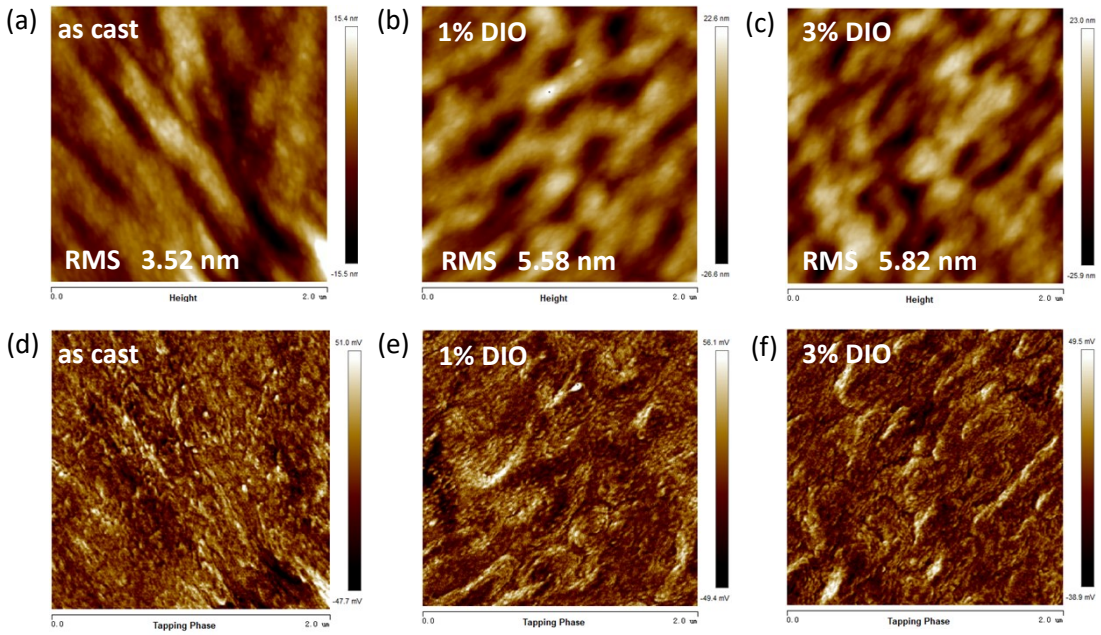

Figure S6. The height (a-c) and phase images (d-f) of the surface in contact with the glass substrates for pure N2200 films with different content of DIO.

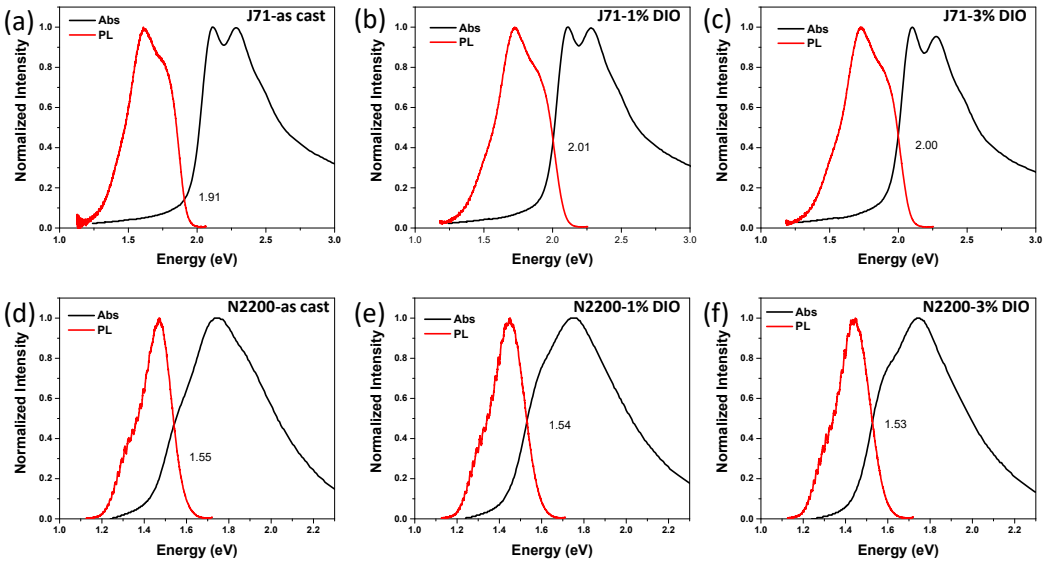

Figure S7. The normalized absorption and PL spectra for pure J71 and N2200 films with different content of DIO, in which the cross point indicates the value of bandgap (E_g).

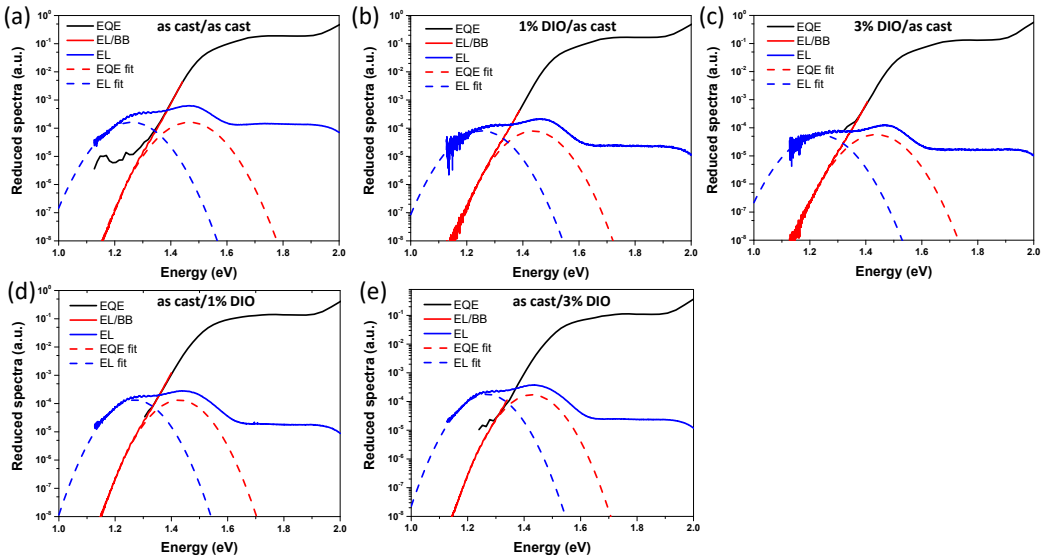

Figure S8. Reduced sensitive EQE and EL spectra of the different bilayer devices.

The CT absorption is typically fitted based on Equation (1):

$$EQE_{PV}(E) = \frac{f}{E\sqrt{4\pi\lambda kT}} exp(\frac{-(E_{ct}+\lambda-E)^2}{4\lambda kT}) \quad (1)$$

where f is associated with the interaction strength between donor and acceptor materials, λ is the reorganization energy during the CT absorption process, kT is thermal energy, and E_{ct} is the CT energy. The overall energy loss of OSCs can be divided into two parts, including the charge transfer energy loss (E_g -E_{ct}) and the charge recombination at CT states (E_{ct} -qV_{oc}). The first part can be obtained by calculated the difference between E_g and E_{ct}. The second part comprises the radiative recombination loss (Δ_{rad}) and non-radiative loss ($\Delta_{non\text{-}rad}$), which can be obtained by the Equation (2) and (3):

$$\Delta_{rad} = -kTln(\frac{J_{sc}h^3c^2}{2\pi fq(E_{ct}-\lambda)}) \quad (2)$$

$$\Delta_{non-rad} = -kTln(EQE_{EL}) \quad (3)$$

where h is Planck constant, c is the vacuum velocity of light, k is Boltzmann constant, T is absolute temperature, and EQE_{EL} is the electroluminescence quantum efficiency.[1-2]

Table S2. The fitted results based on the sEQE and EL curves.

	E_{ct} (eV)	λ (eV)	f (eV)
as cast/as cast	1.36	0.10	4.21E-5
1% DIO/as cast	1.35	0.09	1.91E-5
3% DIO/as cast	1.34	0.10	1.46E-5
as cast/1% DIO	1.35	0.08	2.98E-5
as cast/3% DIO	1.35	0.08	3.89E-5

Table S3. The comparison of interfacial energetic disorder in different systems.

Donor/Acceptor	**Processing conditions**	E_u **(meV)**
PCPDTBT/PCBM (BHJ)[6]	W/O DIO	38.6
	10% DIO	50.7
PTB7:PC_{71}BM (BHJ)[7]	W/O DIO	44
	W/ DIO	42
PTB7-Th:PC_{71}BM (BHJ)[7]	W/O DIO	31.1
	W/ DIO	32.6
J71/N2200 (PHJ)	As cast/As cast	58.1
	3% DIO/As cast	69.2
	As cast/3% DIO	59.5

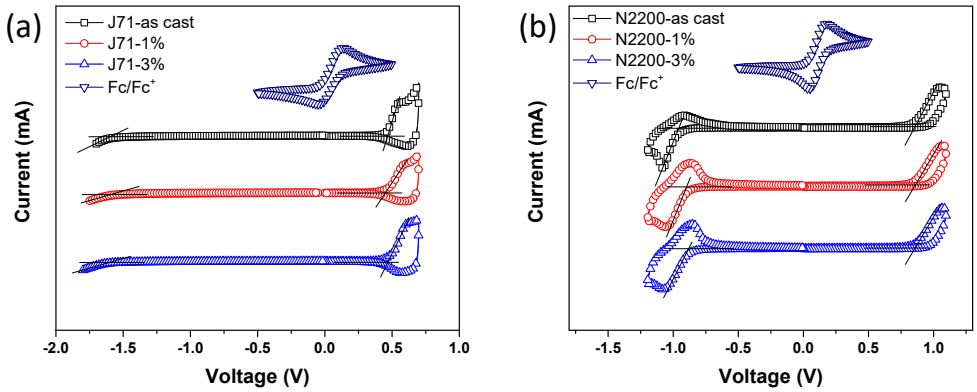

Figure S9. The cyclic voltammetry (CV) curves of pure (a) J71 and (b) N2200 with different content of DIO measured using the Ag/Ag^+ reference electrode.

CV measurements were carried out on a CH-Instruments 650A Electrochemical Workstation. A three-electrode setup was used with platinum wires for both the working electrode and counter electrode, and Ag/Ag^+ was used for the reference electrode calibrated with a ferrocene/ferrocenyl couple (Fc/Fc^+). A 0.1 M nitrogen-saturated solution of tetrabutylammonium hexafluorophosphate (Bu4NPF6) in anhydrous acetonitrile was used as the supporting electrolyte. The energy levels were calculated according to the formula HOMO = − ($E_{onset,ox\ vs.\ Fc/Fc^+}$ + 4.8) eV, where the E_{ox} was determined from the onsets of the oxidation peaks.

Table S4. The specific values of HOMO and LUMO energy for J71 and N2200 films.

		HOMO (eV)	**LUMO (eV)**
J71	as cast	5.27	3.20
	1%	5.25	3.21
	3%	5.26	3.20
N2200	as cast	5.65	3.84
	1%	5.66	3.90
	3%	5.66	3.90

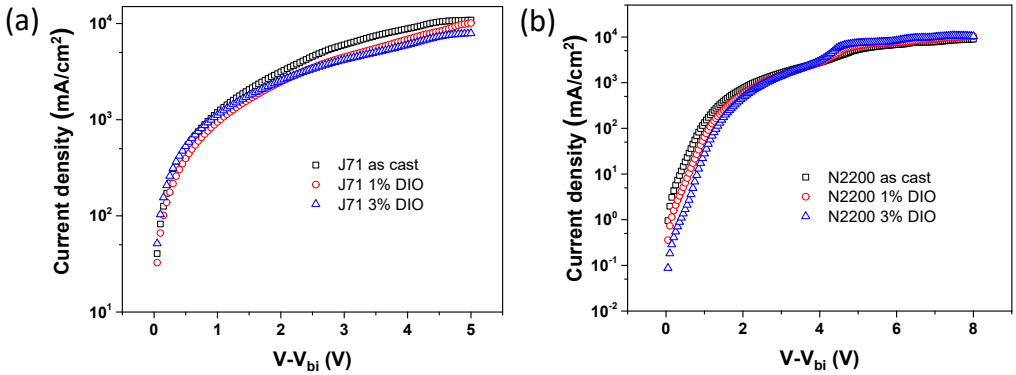

Figure S10. The current density-applied bias voltage curves for (a) hole-only and (b) electron-only devices. The hole-only devices was fabricated with the structure of ITO/PEDOT:PSS/J71/MoO3/Al, while the electron-only devices was fabricated with the structure of ITO/ZnO/N2200/PDINO/Al. The charge carrier mobility was calculated based on the space-charge-limited current (SCLC) model.

Table S5. The calculated hole and electron mobility for the J71 and N2200 films.

J71	**Hole mobility** ($cm^2 V^{-1} s^{-1}$)	**N2200**	**Electron mobility** ($cm^2 V^{-1} s^{-1}$)
as cast	8.84E-5	as cast	4.48E-5
1%	8.01E-5	1%	3.34E-5
3%	5.78E-5	3%	3.01E-5

References:

1. Vandewal, K.; Tvingstedt, K.; Gadisa, A.; Inganas, O.; Manca, J. V., Relating the open-circuit voltage to interface molecular properties of donor:acceptor bulk heterojunction solar cells. *Phys. Rev. B* **2010,** *81*, 125204.

2. Qian, D. P.; Zheng, Z. L.; Yao, H. F.; Tress, W.; Hopper, T. R.; Chen, S. L.; Li, S. S.; Liu, J.; Chen, S. S.; Zhang, J. B.; Liu, X. K.; Gao, B. W.; Ouyang, L. Q.; Jin, Y. Z.; Pozina, G.; Buyanova, I. A.; Chen, W. M.; Inganas, O.; Coropceanu, V.; Bredas, J. L.; Yan, H.; Hou, J. H.; Zhang, F. L.; Bakulin, A. A.; Gao, F., Design rules for minimizing voltage losses in high-efficiency organic solar cells. *Nat. Mater.* **2018,** *17*, 703-709.

3. Jain, N.; Bothra, U.; Moghe, D.; Sadhanala, A.; Friend, R. H.; McNeill, C. R.; Kabra, D. Negative Correlation between Intermolecular vs Intramolecular Disorder in Bulk-Heterojunction Organic Solar Cells, *ACS Appl. Mater. Interfaces* **2018**, *10*, 44576−44582.

4. Jain, N.; Chandrasekaran, N.; Sadhanala, A.; Friend, R. H.; McNeill, C. R.; Kabra, D., Interfacial disorder in efficient polymer solar cells: the impact of donor molecular structure and solvent additives, *J. Mater. Chem. A*, **2017**, *5*, 24749-24757.